



The normal fire environment—Modeling environmental suitability for large forest wildfires using past, present, and future climate normals



Raymond Davis^{a,*}, Zhiqiang Yang^b, Andrew Yost^c, Cole Belongie^d, Warren Cohen^e

^a U.S. Forest Service, Pacific Northwest Region, 3200 SW Jefferson Way, Corvallis, OR 97331, USA

^b Department of Forest Ecosystem and Society, Oregon State University, 3200 SW Jefferson Way, Corvallis, OR 97331, USA

^c Oregon Department of Forestry, 2600 State Street, Salem, OR 97321, USA

^d U.S. Forest Service, National Interagency Fire Center, 3833 South Development Ave, Boise, ID 83705, USA

^e U.S. Forest Service, Pacific Northwest Research Station, 3200 SW Jefferson Way, Corvallis, OR 97331, USA

ARTICLE INFO

Article history:

Received 2 November 2016

Received in revised form 23 January 2017

Accepted 24 January 2017

Keywords:

Fire environment

Climate change

Fire rotation period

PRISM, NEX-DCP30

ABSTRACT

We modeled the normal fire environment for occurrence of large forest wildfires (>40 ha) for the Pacific Northwest Region of the United States. Large forest wildfire occurrence data from the recent climate normal period (1971–2000) was used as the response variable and fire season precipitation, maximum temperature, slope, and elevation were used as predictor variables. A projection of our model onto the 2001–2030 climate normal period showed strong agreement between model predictions and the area of forest burned by large wildfires from 2001 to 2015 (independent fire data). We then used downscaled climate projections for two greenhouse gas concentration scenarios and over 30 climate models to project changes in environmental suitability for large forest fires over the 21st century. Results indicated an increasing proportion of forested area with fire environments more suitable for the occurrence of large wildfires over the next century for all ecoregions but less pronounced for the Coast Range and Puget Lowlands. The largest increases occurred on federal lands, while private and state lands showed less. We calculated fire rotation periods for the recent historical and current climate and examined the relative differences between them and our modeled large wildfire suitability classes. By the end of the century, the models predicted shorter fire rotation periods, with cooler/moister forests experiencing larger magnitudes of change than warmer/drier forests. Modeling products, including a set of time series maps, can provide forest resource managers, fire protection agencies, and policy-makers empirical estimates of how much and where climate change might affect the geographic distribution of large wildfires and effect fire rotations.

Published by Elsevier B.V. This is an open access article under the CC BY-NC-ND license (<http://creativecommons.org/licenses/by-nc-nd/4.0/>).

1. Introduction

Compared to the last three decades of the 20th century, large wildfires in the Pacific Northwest region of the United States have recently been making headlines with increasing frequency. Large forest wildfires account for most of the annual fire suppression expenditures in the western United States and each year cause significant social and economic impacts as well as ecological changes (Ellison et al., 2013; Moritz et al., 2014; USDA, 2015). These wildfires are products of their environment and the forested environments of the western US appear to be coming more suitable for their occurrence due to climate change (Abatzoglou and Williams, 2016; Westerling, 2016). Climate is one of the modifying forces of the fire environment that interacts with topography and

fuel (e.g., a layer of live and dead vegetation available for burning); each component conceptually forming a side of the “fire environment triangle” (Countryman, 1972: p. 5). This decades-old concept appeared a few years before the concept of the “ecoclimatic triangle” (Hustich, 1978: Fig. 1) that described the interaction between human activities, the climate, and the environment. We combined both concepts to extrapolate and contrast what we consider as today’s “normal” fire environment to what might be considered normal by the end of this century as a result of forecasted changes in climate. Here, the term “normal” implies the typical state based on averaged conditions from a geographic area over decades of time (Lutz et al., 2011; Trewin, 2007).

Empirical studies describing environmental gradients that influence geographic patterns of wildfire over broad landscapes and how climate change may affect those gradients are becoming more commonplace (Krawchuk et al., 2009; Krawchuk and Moritz, 2014; Liu and Wimberly, 2016; Moritz et al., 2012;

* Corresponding author.

E-mail address: rjdavis@fs.fed.us (R. Davis).

Parisien and Moritz, 2009; Parisien et al., 2012). Such assessments help improve our understanding of the effects of changing environmental controls on the geography of fire. Mutual to all of these modeling efforts is the use of the aforementioned three environmental components. Temporally, of the three, topography is the most stable, taking centuries to millennia to change; whereas, burnable vegetation (fuel) is dynamic and can change from year to year in response to disturbance and growth processes. Climate normals change at a rate in between these two temporal frequencies (e.g., decades). Given recent observed changes in climate and projections of changes in the future, the climate component of the fire environment is a major focus of research.

It has long been known that climate largely determines “the nature of the wildfire problem” and the resulting fire management policies and resources needed (Reifsnyder, 1960). Thus, a changing climate implies a need for a change in fire management policies and strategies (North et al., 2015). Understanding the conditions that produce suitable environments for large forest wildfires and how those conditions are expected to change with increasing concentrations of greenhouse gases in the atmosphere is critical for a better understanding of where large wildfires are likely to occur now and into the future (Parisien and Moritz, 2009). Reliable temporal and spatial predictions of large wildfire suitability in forested ecosystems are essential for correctly identifying and managing threats to valued resources, prioritizing forest management, and wildfire protection. The need for such assessments is vital in the socially, economically, and ecologically important coniferous forests of the Pacific Northwest (PNW) region of the United States where several studies have predicted large wildfires will occur more frequently and burn larger in the future (Flannigan et al.,

2000; Moritz et al., 2012; Rogers et al., 2011; Stavros et al., 2014). Indeed, an increasing frequency of large forest wildfire occurrence and area burned has already been observed in this region (Dennison et al., 2014; Littell et al., 2009). The objectives of this study were to: (1) characterize the most recent normal fire environment for the forests within Region 6 of the USDA Forest Service (Oregon and Washington); (2) to project this environmental relationship into the future under varying climate change scenarios and; (3) examine the differences between today’s normal fire environment and those of the possible futures.

2. Data and methods

2.1. Study area

Our study area covered 216,900 km² of forest land in Washington and Oregon. Slightly more than half (52%) is managed by the Federal Government. The United States Department of Agriculture Forest Service (USFS) manages about 91,200 km² on 16 National Forests, the United States Department of Interior (USDI) Bureau of Land Management (BLM) manages about 14,000 km², the USDI National Park Service (NPS) manages about 6700 km², and a mix of other federal agencies manage another 800 km². Privately owned forests comprise about 38% (~81,500 km²) while the remaining 10% is comprised of State and Local Government (~13,600 km²) and Tribal Lands (~9100 km²).

There are eight EPA Level III ecoregions (Omernik and Griffith, 2014) in the study area that contain large areas of forestland encompassing a wide range of floristic, physiographic and climatic variability (Fig. 1). Forests vary from the moist Sitka spruce (*Picea*

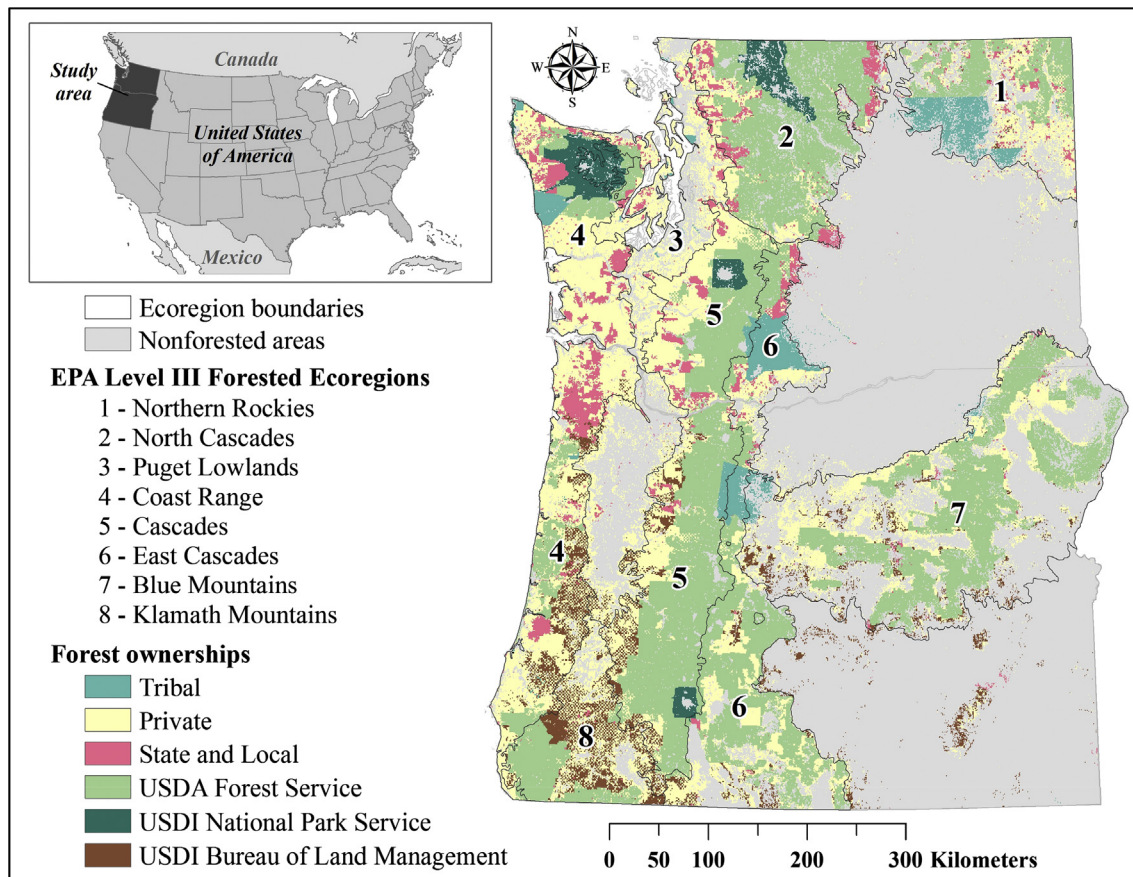


Fig. 1. Study area map showing the major forested ecoregions and major forest ownership patterns.

sitchensis) and western hemlock (*Tsuga heterophylla*) rain forests of the coastal region to mixed conifer, dry ponderosa pine (*Pinus ponderosa*) and western juniper (*Juniperus occidentalis*) east of the Cascades; and from lowland Douglas-fir (*Pseudotsuga menziesii*) forests to high elevation Pacific silver fir (*Abies amabilis*), mountain hemlock (*Tsuga mertensiana*), and subalpine fir (*Abies lasiocarpa*).

The current climate to the west of the Cascade Mountains is mostly temperate maritime grading to Mediterranean in south-western Oregon. Warmer and drier temperate conditions occur from west to east across the Cascade Mountains with vegetation transitioning from coniferous forests to large areas dominated by arid steppe/desert ecosystems. During the climate normal period from 1971 to 2000, mean monthly forest precipitation from May to September ranged from 12 to 201 mm (Table 1). This is the time of year when most large forest wildfires have occurred in this region (Barbero et al., 2014). The average monthly maximum temperature during the peak months of the wildfire season (July to August) ranged from 12 to 33 °C (Table 1).

The forests managed by the BLM had the warmest/driest fire season climate based on the 1971–2000 climate normal data, whereas the coolest/moistest fire season climate occurred on NPS forests (Table 2). State, local, and private forests occur at the lowest elevations on average, while forests managed by the NPS and USFS occur in the highest elevations on average. Forests on private and tribal-owned lands tended to have gentler slopes (Table 2).

2.2. Environmental variables

Our modeling focused on the intrinsic elements of the fire environment (Countryman, 1972); vegetation (fuel) available for burning, climate, and topography. Forested areas mapped by the USFS Forest Inventory and Analysis Program (Ruefenacht et al., 2008) represented the “fuel” side of the fire environment triangle. While considerable efforts have been made to map geographic patterns of

forest fuel models, it remains difficult at best (Arroyo et al., 2008; Keane, 2013) and their patterns are highly dynamic and constantly changing. Predicting fine scale future patterns of fuel accurately would include a very high amount of uncertainty and may not be feasible. For that matter, predicting the broader patterns of forest type dynamics under a changing climate also involves a great deal of uncertainty (Peterson et al., 2014; Purves and Pacala, 2008). Therefore, we assumed that the current forested areas will, on average, provide burnable fuels and a stable forest footprint over the course of this century.

Wildfire studies in Pacific Northwest forests have shown strong correlations between fire occurrence and area burned with summer temperature and precipitation (Davis et al., 2011; Littell et al., 2010; McKenzie et al., 2004). Our climate variables were temperature and precipitation climate normals that coincided with the most active months of the study area’s fire season, thus directly influencing fire behavior and suppression efforts which factor into a fire’s growth. Climate normals were based on 30-year weather averages and used as references of conditions likely to be experienced at a given location (Trewin, 2007). Precipitation (hereafter referred to as PPT) was calculated as the 30-yr mean for the months from May through September, and temperature (TMAX) was calculated as the 30-yr mean of the maximum temperature for July and August, which coincides with the peak months of the fire season. Information sources for PPT and TMAX representing the recent climate normal from 1971 to 2000 and the currently used climate normal 1981–2010 (hereafter; current climate normal) came from datasets (30 arc-sec, ~800 m spatial resolution) generated by the Parameter-elevation Regressions on Independent Slopes Model (Daly et al., 2008; PRISM, 2015). Future climate normals were derived from the NASA Earth Exchange downscaled climate projections (NEX-DCP30) dataset for the US, which used PRISM as its observational climate data to develop the model used in creating future climate datasets that also matched the spatial

Table 1

Summary of forest topography and fire season climate by forested ecoregion. Temperature and precipitation are seasonal norms (1971–2000), not annual. Topographic variables were resampled to match the 800 m² spatial resolution of the climate data. Ecoregions were ordered (top to bottom) from warmer/drier to cooler/moister fire season climates.

Forested ecoregion	Elevation (m)			Slope (%)			Temperature ^a (°C)			Precipitation ^b (mm)		
	Min	Max	Mean	Min	Max	Mean	Min	Max	Mean	Min	Max	Mean
Klamath Mountains	64	2125	705	1	84	37	19	32	28	15	112	38
East Cascades	26	2456	1375	0	74	15	17	31	26	12	78	25
Blue Mountains	405	2854	1413	0	102	25	15	33	26	14	78	33
Northern Rockies	396	2048	1027	0	75	26	17	31	25	20	112	46
Puget Lowlands	0	1518	159	0	89	11	16	26	24	21	119	53
Cascades	19	2347	1004	0	108	31	15	32	24	19	142	66
Coast Range	0	1599	311	0	114	32	15	30	23	24	197	72
North Cascades	28	2388	1176	0	141	47	12	31	21	13	201	72

^a Mean monthly maximum temperature for July and August.

^b Mean monthly precipitation from May thru September.

Table 2

Summary of forest topography and fire season climate by major forest ownership. Temperature and precipitation are seasonal norms (1971–2000), not annual. Topographic variables were resampled to match the 800 m² spatial resolution of the climate data. Ownerships were ordered (top to bottom) from warmer/drier to cooler/moister fire season climates.

Forest ownership	Elevation (m)			Slope (%)			Temperature ^a (°C)			Precipitation ^b (mm)		
	Min	Max	Mean	Min	Max	Mean	Min	Max	Mean	Min	Max	Mean
USDI Bureau of Land Management	0	2629	875	0	95	31	17	33	27	10	119	37
Tribal	0	2251	910	0	74	20	16	32	25	9	131	36
Private	0	2366	626	0	117	22	16	33	25	8	187	50
USDA Forest Service	0	2854	1283	0	137	33	14	32	24	12	201	53
State and Local	0	2222	608	0	122	30	15	32	24	9	190	68
USDI National Park Service	0	2294	1148	0	141	53	12	30	20	21	193	86

^a Mean monthly maximum temperature for July and August.

^b Mean monthly precipitation from May thru September.

resolution and attributes of PRISM (Nemani et al., 2011; Thrasher et al., 2013). The datasets we used included downscaled climate projections from 33 general circulation models (GCMs) for representative concentration pathway (RCP) 4.5 and 31 GCMs for RCP 8.5 (Van Vuuren et al., 2011) under the Coupled Model Intercomparison Project (CMIP) Phase 5 (Taylor et al., 2012). RCP 4.5 assumed moderate global mitigations to reduce greenhouse gas emissions and an increase in forested areas; where atmospheric concentrations peaked by mid-century then began to stabilize, but at higher than current levels (Thomson et al., 2011). RCP 8.5 assumed no mitigations and a decrease in global forested areas resulting in increasing greenhouse gas concentrations throughout the 21st century (Riahi et al., 2011). We did not use RCP 2.6 and 6.0, because the available NEX-DCP30 datasets for these two RCPs had only 17 of 33 GCMs in common, whereas RCP 4.5 and 8.5 had 31. Thus, making comparisons between RCPs more relevant to differences between the scenarios as opposed to differences due to the suite of GCMs used. Future climate normals for each GCM under each RCP were calculated in Google Earth Engine (Gorelick, 2013) (<https://earthengine.google.org/>).

Topographic variables included slope as percentage (SLP) and elevation in meters (ELEV), resampled to match the spatial resolution of our climate variables using bilinear interpolation from 30×30 m resolution digital elevation models. There was a moderate negative correlation between TMAX and PPT ($r = -0.6$); however, the variance inflation factors (VIF) for all four model variables ranged from 1.2 to 2.2. Both of these measures were lower than commonly used modeling thresholds ($r > 0.7$ and $VIF > 10$) where collinearity begins to confound model performance (Dormann et al., 2013).

There are a host of other factors that can help to explain the occurrence of wildfire, both environmental (e.g., historical lightning ignition density) and anthropogenic (e.g., distance to roads) (see Appendix G in Davis et al., 2011). Anthropogenic factors can have a noticeable influence on fire probability models (Mann et al., 2016), however assumptions on how these human factors will change into the future from patterns observed today is problematic. Here, we selected a simple set of environmental variables that not only fit the basic components of the fire environment triangle, but have also already been modeled and mapped into the future.

2.3. Large wildfire data

We used large forest wildfire occurrence data within our study area (Fig. 2) that was coincident with the climate normal from

1971 to 2000 to train and test our baseline fire environment model. We used large forest wildfires from 2001 to 2015 to further evaluate our models with data independent of the model training process. Following the standard established by the USDA Active Fire Mapping Program (<https://fsapps.nwccg.gov/afm/>) we considered forest wildfires at least 40 ha in size as a “large” wildfire. During the three decades of the baseline time period a total of 512 large wildfires burned a total area of 7400 km², of which about 4900 km² were forested. In half that time, 651 large wildfires burned slightly over 3 times the amount (16,100 km²) of forest between 2001 and 2015 (Fig. 2).

From the baseline data we generated point locations on the center of each $800 \text{ m} \times 800 \text{ m}$ (64-ha) pixel within the perimeter of all wildfires that contained at least 5% forested area. To minimize spatial autocorrelation effects in our model training we randomly sampled from these center locations using an area-based algorithm where the number of points per wildfire was proportional to the square root of the ratio between the area burned to the area of the smallest wildfire. As a result, the smallest wildfire (40 ha) was represented by only one point, and the largest wildfire (56,726 ha) was represented by 37 random points separated by at least 800 m. This reduced our sample locations from 7724 to 1967.

2.4. Modeling the fire environment

We used MaxEnt version 3.3 (Phillips et al., 2006; Phillips and Dudík, 2008) to model the fire environment of the 1971–2000 climate normal period. MaxEnt uses a machine learning method and the principle of maximum entropy to fit mathematical functions of environmental predictor variables to presence locations (the response variable). It does so by maximizing the likelihood ratio of average presence values to average values from a large random sample of the background environment (Merow et al., 2013). Machine learning methods are increasingly being used to empirically model fire environment relationships (De Angelis et al., 2015; West et al., 2016). These approaches differ from process-based methods by allowing for model calibration and evaluation with actual fire observational data to enhance model accuracy, identify uncertainties, and build model credibility (Alexander and Cruz, 2013).

Our objective was to build a baseline model with an appropriate balance between simplicity and complexity to describe the general relationship between large wildfire occurrence and fire environment variables (Bell and Schlaepfer, 2016; Elith et al., 2011; Merow et al., 2014). Thus, we limited our model fitting options

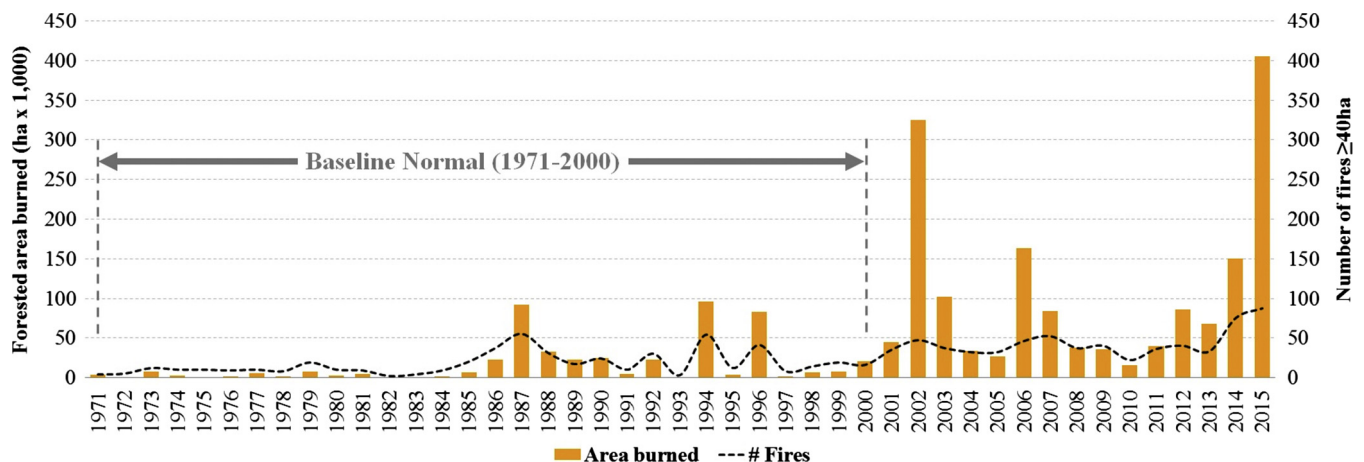


Fig. 2. Large (≥ 40 ha) forest wildfire history for the study area. The black dashed line for number of fires was smoothed.

to linear, product, or quadratic functions. This combination of functions is reflected in the model output predictor response curves that show the relationship between environmental suitability for large wildfire occurrence (y-axis) and the range of values for each predictor variable (x-axis). We expected that the relative environmental suitability for large wildfires would generally increase with increasing TMAX. We anticipated that suitability would increase with ELEV due to its relationship with lightning strike densities and ignitions (Dissing and Verbyla, 2003; Preisler et al., 2004; van Wagtenonk and Cayan, 2008). We expected to see a positive relationship with SLP and a negative relationship with PPT. Finally, to prevent model projections from assuming empirical relationships for future predictor variables values outside of the range used to train the baseline model we used variable clamping, which keeps the response function flat for values above or below the training data (Phillips et al., 2006). Clamping, however, may result in poorer representation of environmental relationships for climatic conditions outside of the model training dataset so further examination of response functions for this situation is warranted (Bell and Schlaepfer, 2016).

We generated 50 bootstrapped model replicates, each time randomly selecting half ($n = 984$) of the large wildfire data locations and 10,000 random locations from other forested 800 m pixels within the modeling region. The remaining half ($n = 983$) of the large wildfire data were used to evaluate model performance. The model was calibrated with stepwise incremental adjustments (0.5) of a regularization multiplier (RM). The RM is an algorithm coefficient based on a combination of likelihood with a complexity penalty, making it conceptually similar to AIC (Burnham and Anderson, 2002; Merow et al., 2014). For each RM increment, we examined model training and test gains that indicate model overfitting when test gains are significantly lower than training gains. We also examined the test area under the receiver operating characteristic curve (AUC) statistic (Swets, 1988) and the continuous Boyce index (CBI), both of which are used to evaluate model accuracy and fit to the testing data (Boyce et al., 2002; Fielding and Bell, 1997; Hirzel et al., 2006). We selected the model that achieved similar training and test gains, while maximizing test AUC and CBI statistics.

We projected the baseline model onto similar predictor data for the current climate normal (PRISM 1981–2010) and future climate normals using NEX-DCP30 data (1991–2020, 2001–2030 ... 2071–2100). We produced 33 future fire environment models for RCP 4.5 and 31 models for RCP 8.5 for each normal period. Each of these models was based on a different GCM. We used the median and absolute deviation maps from these various GCMs for each RCP as the basis for depicting and evaluating the spatial changes of the fire environment from current to the end of the century.

2.5. Mapping and validating large wildfire suitability

To facilitate model interpretation we used the predicted-to-expected (P/E) curve from the CBI analysis to reclassify our baseline model into three large wildfire suitability classes (Hirzel et al., 2006; Fig. 6). The P/E curve represents the ratio of the proportion of test locations (P) that occurred within a “moving window” width of 0.1 along the predicted suitability axis (x-axis) to the proportion of the model region available for fire occurrence (E) within that same window. A good model is indicated by a monotonically increasing P/E curve. Low suitability was classified as $P/E < 1$, indicating that the model predicted large wildfire occurrence less than would be expected by random chance. Moderate suitability was classified as $P/E > 1$ to the step of the curve where the P/E ratio begins to exhibit a noticeable positive increase (Hirzel et al., 2006). High suitability was classified as the area above this step threshold.

Using a method described in Moreira et al. (2001) we evaluated model performance for projecting the baseline model onto future climate normals. Specifically, using the 2001–2030 projected map we calculated the ratio of the proportion of the forest that was burned by large wildfires for each year from 2001 to 2015 to the proportion of the forested area that was available for burning in each large wildfire suitability class. The interpretation of this burned-to-available for burning (B/A) ratio is similar to the P/E ratio; a value of $B/A < 1$ indicates that the map class burned less than would have been expected by chance and a ratio $B/A > 1$ indicates it burned more than would be expected by chance. For each suitability class, B/A ratios were averaged across years and confidence intervals were constructed. The chi-square goodness of fit test (Byers et al., 1984) was used to test for significant B/A ratio differences between large wildfire suitability classes.

2.6. Estimating changes in fire rotation periods

We calculated the fire rotation period (FRP) for each large wildfire suitability map class for both the baseline and current climate normal periods using the burned area-based equation (eqn. 7) from Li (2002). These FRPs were estimated for 30-year time periods and not expected to represent natural fire cycles owing to fire suppression, especially in the low suitability class where large fires are rare for any given 30-yr period. Rather, they represent observed FRPs. Given that FRPs vary widely across time (Li, 2002) we calculated the relative difference between fire suitability classes for both time periods. We used the averaged class differences to estimate the relative magnitude of FRP change, based on class transitions (e.g., low to moderate) from the current climate normal to the climate normal period at the end of this century.

3. Results

3.1. Fire environment modeling

Our best model was produced using a RM setting of 2.0, with a CBI of 0.97 ± 0.02 and a test AUC of 0.77 ± 0.01 . All modeled RM versions had similar average training and test gains (0.48 ± 0.1 and 0.49 ± 0.1 , respectively; means and 95% confidence limits) indicating that model overfitting was not an issue. Predictor variable model average contributions were similar for all RM versions, with TMAX consistently being the strongest predictor ($41.0 \pm 1.2\%$), followed by ELEV ($28.1 \pm 0.5\%$), PPT ($20.1 \pm 1.4\%$), and SLP ($10.7 \pm 0.2\%$). There was little variation in area predicted as suitable ($39.9 \pm 0.7\%$) among RM settings, indicating a high level of model robustness.

Response curves were consistent with expected relationships for each of the predictor variables (Fig. 3). Relative environmental suitability for large wildfires increased with increasing TMAX and decreased with the increasing PPT. It was also positively related with ELEV and SLP, meaning that forests at higher elevations and on steeper slopes are more likely to experience large wildfires. However, suitability decreased on extremely steep slopes (>90%) perhaps in relationship to cliffs and other rocky features associated with steep terrain that lack fuel or may act as physical barriers to fire spread (Beatty and Taylor, 2001; Clarke, 2002).

3.2. Wildfire suitability map classes and validation

The final baseline model predicted relative occurrence of large wildfires accurately based on the monotonic increase of the P/E curve when plotted against the range of suitability values (Fig. 4). The P/E curve steadily increased from 0 to 1 for large wildfire suitability (LWS) values from 0 to 0.37 and continued to

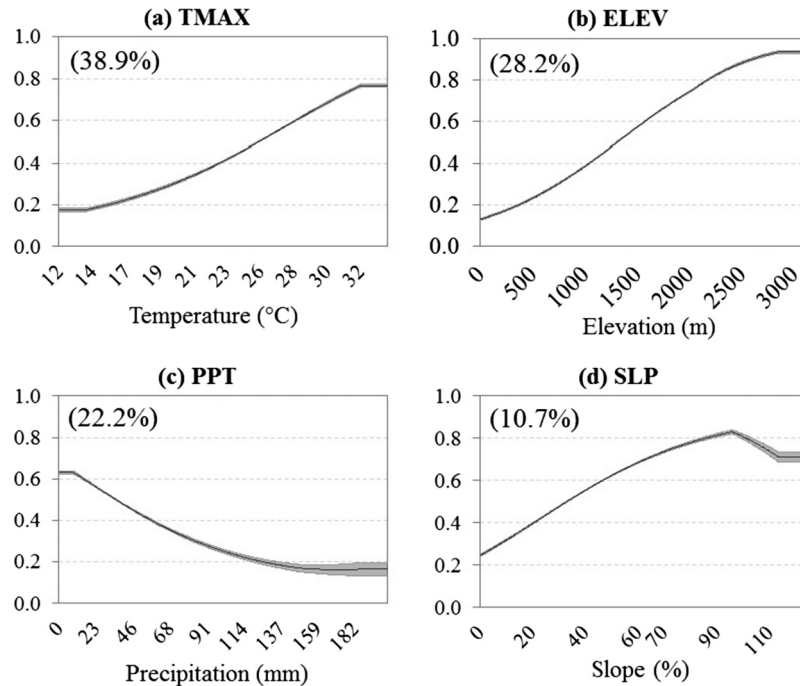


Fig. 3. Modeled fire environment variable response functions and percentage contributions in parentheses. July–August maximum temperature (a) was the strongest variable, followed by elevation (b), May–September precipitation (c), and slope (d). Solid lines are means and shaded areas are 95% confidence intervals from bootstrapped replicates (n = 50). Horizontal ends indicate variable clamping.

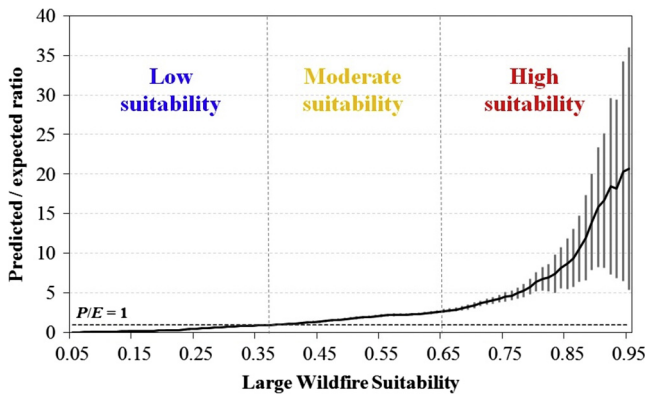


Fig. 4. The predicted versus expected (P/E) curve. Solid black line shows the mean from 50 replicates, vertical gray bars show 95% confidence intervals. The horizontal black dashed line represents the value expected if the model prediction were no better than random chance ($P/E = 1$). The vertical gray dashed lines show suitability map class thresholds.

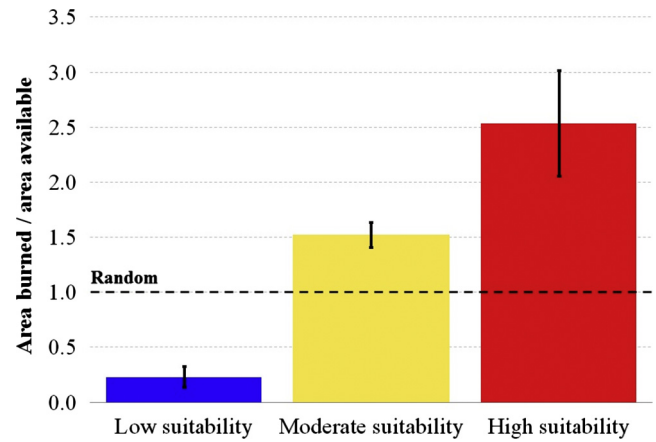


Fig. 5. Histogram of the burned-to-available for burning (B/A) ratios for forests burned from 2001 to 2015 (independent test data) using the 2001–2030 normal fire environment map. Bars represent map class averages with 95% confidence limits.

increase as LWS increased to 0.65. Above this point the P/E curve began to increase exponentially, reflecting better model discrimination. The final model was very robust with tight confidence intervals up to LWS = 0.8. The variation between bootstrapped replicates increased past this point, but confidence intervals never fell below the $P/E = 1$ threshold (Fig. 4).

Based on the chi-square goodness-of-fit test ($\chi^2 = 5069$; $P < 0.001$) the proportion of forest that burned on average for each year between 2001 and 2015 in each wildfire suitability class predicted by the model was significantly different than expected under the hypothesis that proportion of forest area burned was relative to the amount available. Forests mapped as low suitability burned on average five times less than would be expected by chance (0.2), moderately suitable forests burned about 1.5 times more than would be expected, and high suitability forests burned

about two to three times higher than would be expected by random chance (Fig. 5).

3.3. Climate change predictions

NASA Earth Exchange downscaled climate models (NEX-DCP30) predicted warmer and drier fire seasons for the forests of Oregon and Washington by the end of this century. Climate normals for TMAX increased on average across all forests within the study area by 3.5 and 6.2 °C under RCP 4.5 and 8.5, respectively (Fig. 6a). Climate normals for PPT decreased by 2.8 and 5.4 mm under RCP 4.5 and 8.5, respectively (Fig. 6b). Changes in the spatial extent of novel (outside of what has been observed within the study area in the PRISM data) future forest climate conditions occurred mainly for TMAX and exceeded 5% of the forested area by the

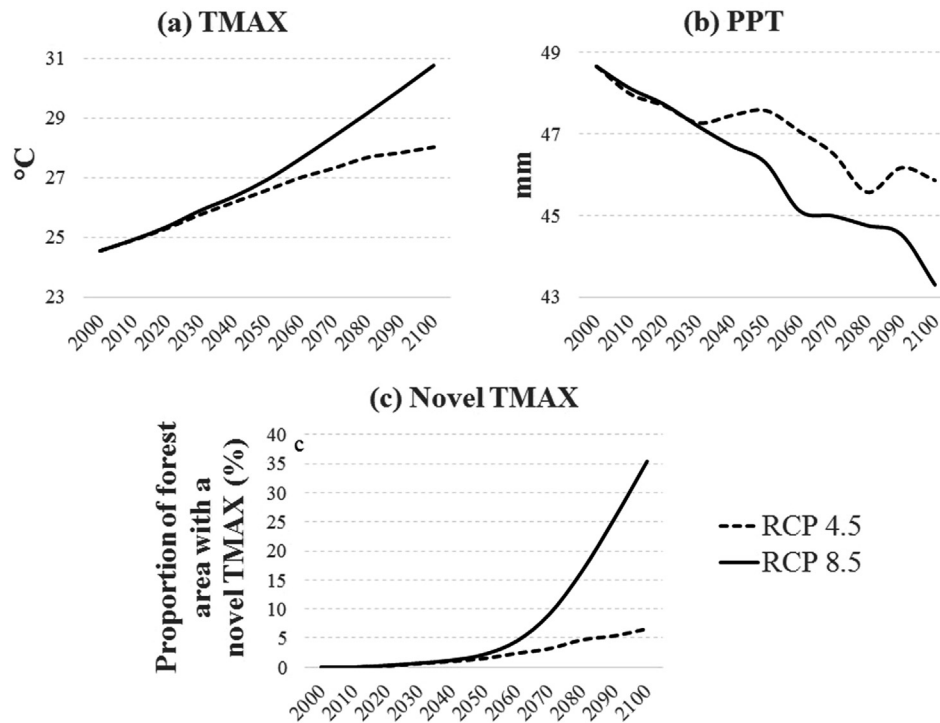


Fig. 6. Median NEX-DCP30 GCMs showed (a) varying patterns of increasing mean July-August temperature TMAX (b), decreasing mean May-September precipitation PPT, and (c) increasing areas with novel TMAX over time across the forests of Oregon and Washington under RCP 4.5 and 8.5, by the end of this century.

2041–2070 climate normal period (under RCP 8.5), when it begins to rapidly increase (Fig. 6c). Novel changes in PPT were discountable in spatial extent (<1% of forested area).

During the baseline climate normal (1971–2000), about 59% of the forests within the study area were classified as having a fire environment that was of low suitability, 36% as moderately suitable, and 5% as highly suitable for the occurrence of large wildfires. Projection of the model onto the current climate normal period (1981–2010) showed a 1.6% decrease of forested area classified as low suitability and a 1.6% increase in highly suitable forests while the area of moderately suitable forests remained constant. For future projections, a similar pattern emerged for both RCPs. As low suitable forests transitioned into moderate and moderate transitioned into high, the area of forests classified as low suitability shrank while forests classified as high expanded and moderately suited forest area remained more or less the same (Fig. 7). Under RCP 4.5 the percentage of forests classified as low suitability decreased from the current 57% to 38% by the end of the century and forests classified as highly suitable increased from 7% to 27%. Under RCP 8.5 the percentage of low suitability forests decreased from the current 57% to 37% and highly suitable forests increased from 7% to 31%. In general, median relative suitability increased through time under both RCPs and across all forest ecoregions. Uncertainty in model predictions varied geographically and generally increased with time. Median absolute deviations were highest in the Cascades and lowest in the Puget Lowlands ecoregion (Fig. 7).

3.4. Fire suitability trend by ecoregions

The proportion of forests predicted to transition from one large wildfire suitability class to another by the end of the century varied among ecoregions (Fig. 8). All ecoregions, with the exception of the Puget Lowlands, showed increases in the proportion of forests modeled as highly suitability for large wildfire occurrence by the

end of the century under both RCP scenarios. The largest increase was in the Blue Mountains ecoregion, where the proportion of high suitability forest increased from the current extent of 17% to 63–72% (RCP 4.5 and RCP 8.5, respectively). This was followed (in decreasing order of magnitude) by the Klamath Mountains; from 18% to 48–51%; the East Cascades, from 11% to 40–45%; the North Cascades, from 2% to 28–33%; the Northern Rockies, from <1% to 17–26%; the Cascades, from 1% to 13–18%; and the Coast Range, where it increased slightly from <1% to 2% under both RCPs.

The proportion of forests with low suitability fire environments decreased in all ecoregions. The largest decrease was in the Northern Rockies from the current extent of 67% to 20–14% (RCP 4.5 and RCP 8.5, respectively). This was followed (in decreasing order of magnitude) by the North Cascades, from 63% to 35–32%; the Cascades, from 71% to 47–44%; the East Cascades, from 21% to 5–4%; the Klamath Mountains, from 30% to 14% (both RCPs); the Coast Range, from 97% to 85% (both RCPs); the Blue Mountains, from 9% to <1% (both RCPs); and the Puget Lowlands, which decreased slightly from 100% to 99% under both RCPs (Fig. 8).

3.5. Fire suitability trend by ownership

Forests with fire environments highly suitable for large wildfire occurrence were projected to increase across all ownerships (Fig. 9). The largest increase was on forests managed by the USFS where the proportion of high suitability forest increased from the current extent (9%) to 39–44% (RCP 4.5 and RCP 8.5, respectively) by the end of this century. This was followed (in decreasing order of magnitude) by BLM, from 18% to 45–49%; Tribal-owned forests, from 2% to 22–25%; Private forests, from 4% to 17–20%; NPS, from 1% to 10–13%; and State forests; from 1% to 10–12% (Fig. 9).

Conversely, the geographic extent of low suitability forests was projected to decrease on all ownerships with extent of decrease larger for RCP 8.5. The largest decrease was in forests managed by the NPS, which currently has the highest proportion of low suit-

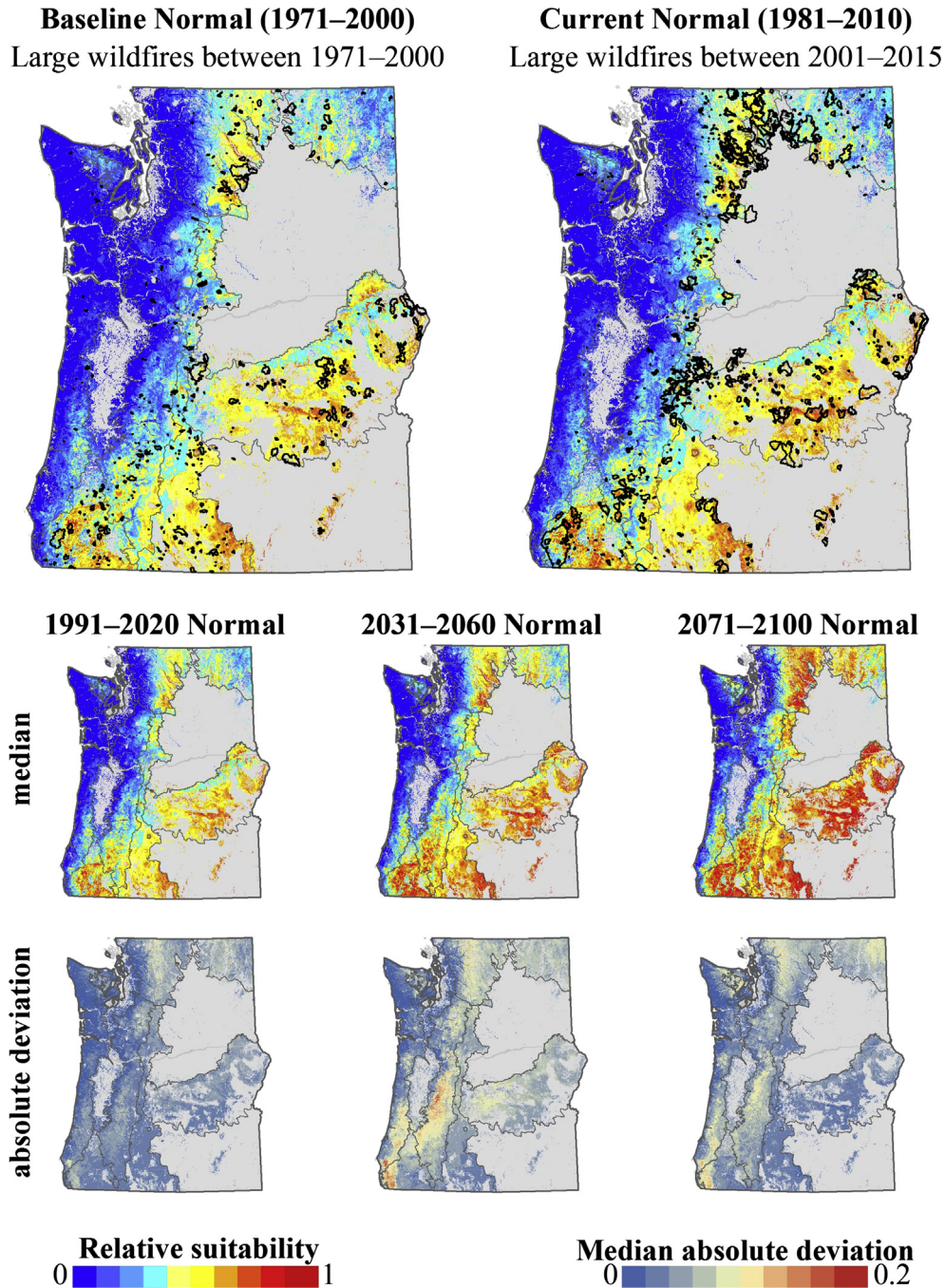


Fig. 7. Fire environment maps derived from PRISM data showing large wildfires from the baseline normal period (1971–2000) and current normal period (1981–2010) (top maps). Future fire environment time series maps (1991–2020, 2031–2060, and 2071–2100) derived from NEX-DCP30 data show predicted change under RCP 8.5. Median absolute deviation maps for each of these time periods provide information on how much and where model predictions varied.

ability forest. This extent was predicted to decline from 86% to 46–45% (RCP 4.5 and 8.5, respectively) by the end of the century. This was followed (in decreasing order of magnitude) by Tribal-owned forests, from 56% to 24–23%; forests managed by the USFS; from 42% to 20–19%; State forests; from 82% to 69–67%; BLM forests, from 38% to 21–18%; and Private forests, from 70% to 58–56%. By the end of the century, State and Private forests were predicted to have the highest proportions of low suitability forest.

3.6. Changes in fire rotation periods

Due to an increase in forest area burned in recent years, fire rotation periods have already decreased between the baseline

and current climate normal periods. FRPs were longest for the low suitability forests (5291 and 1894 years), intermediate for the moderate suitability forests (703 and 274 years), and shortest for high suitability forests (355 and 169 years) for the baseline and current normal periods, respectively. The averaged differences in FRPs for moderate suitability forests was 2-times shorter than in high suitability forests. In low suitability forests, it was 7-times shorter compared to moderately suitable forests, and 13-times shorter compared to highly suitable forests. Under both RCPs, about 19–20% of low suitability forests transitioned into moderately suitable forests, 20–24% from moderate to high, and less than 1% from low to high by the end of the century. About 55–61% of the forested area remained in their current suitability class (Fig. 10).

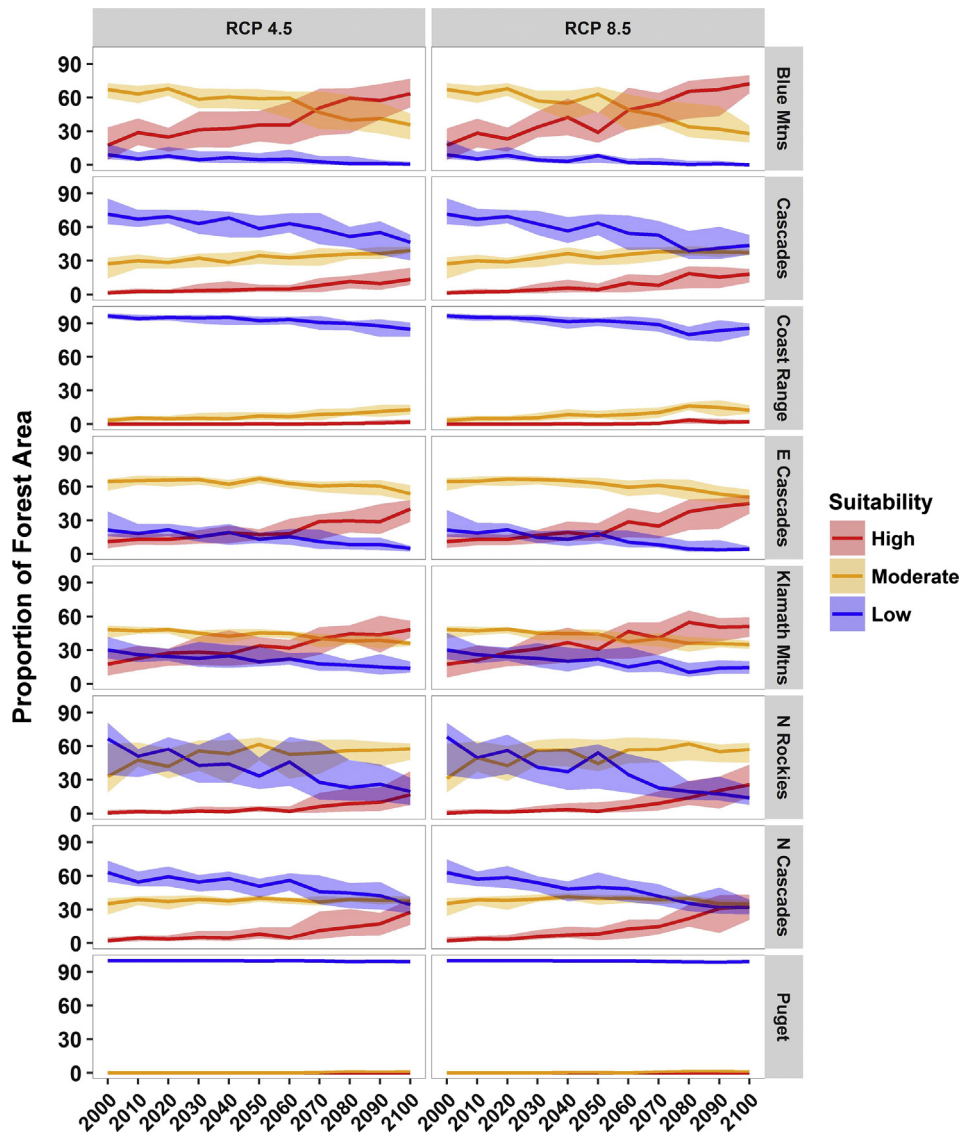


Fig. 8. Predicted trends in large wildfire suitability by forested ecoregion. Solid lines represent the median proportion from all GCM maps. Shaded areas represent the quartile range.

On average the FRP was shortened the most in the Northern Rockies ecoregion by a factor of 3.6 to 4.1 (RCP 4.5 and 8.5, respectively) followed by a twofold decrease in the Cascades ecoregions (Table 3). Forests managed by the BLM and USFS showed a 3-fold decrease in FRPs by the end of the 21st century, while forests managed by the state and local government had the lowest decrease in FRP (Table 3). Across the entire study area, FRP decreased by a factor of 2.4–2.7 (RCP 4.5 and 8.5 respectively).

4. Discussion

4.1. Fire environments under climate change

The modeling described here combined new methods and old concepts to produce a time series of maps that showed how large wildfire environments might change within the forests of Oregon and Washington under differing climate change scenarios. We focused on fundamental environmental controls to represent the intrinsic nature of the fire environment. We utilized state-of-the-art empirical modeling methods to produce a simple, intuitive model. Three decades of large forest wildfire data from the last

century were used to train the model and large wildfire data from the first 15 years of this century were used to independently test it. The model predicted well where large forest wildfires are most likely to occur. Our modeling approach was similar to a recent conceptual model of the “fire regime triangle”, consisting of three components; (1) resources to burn, (2) conditions suitable for burning, and (3) an ignition agent (Krawchuk and Moritz, 2014). The “core” of the fire regime triangle is defined by long-term environmental norms or averages, but fire activity can be complemented by inter-annual environmental fluctuations (Krawchuk and Moritz, 2014). Under this concept, our normal fire environment model perhaps best represents the core of the fire regime triangle.

Climatic variables explained 61.1% of our baseline fire environment model. Peak fire season maximum temperature (TMAX) was the strongest variable and increased on average across the study area by 3.5 and 6.2 °C by the end of this century (under RCP 4.5 and 8.5, respectively). Fire season precipitation (PPT) was predicted to decrease on average by 2.8 and 5.4 mm. Regional novel future forest climate conditions occurred primarily for TMAX and were small and negligible for PPT, consistent with other studies

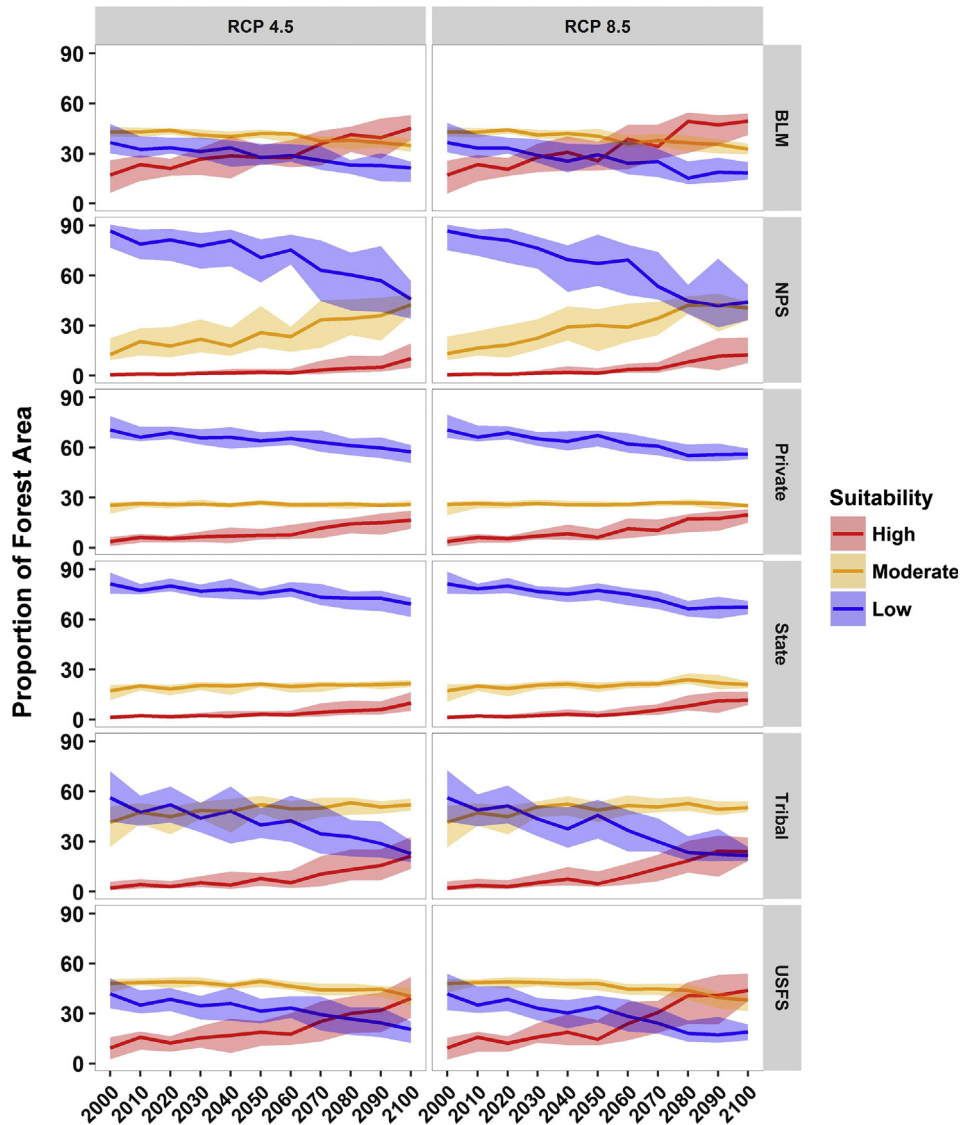


Fig. 9. Predicted trends in large wildfire suitability by forest ownership. Solid lines represent the median proportion from all GCM median maps. Shaded areas represent the quartile range.

(Mote and Salathe, 2010). The variation in percentage of forests predicted to transition from one large wildfire suitability class to another by the end of the century was large across ecoregions and ownerships. Percentages of forest predicted to transition to higher suitability classes in the coastal ecoregions were lowest for the Puget Lowlands with a slight increase in the moderate class and the Coast Range, where a relatively small amount of low suitability forests transitions to a high suitability. Under RCP 8.5 forests classified as low suitability were predicted to disappear from the Blue Mountains transitioning to moderate and high suitability classes. The area of forested land classified as highly suited for large wildfires was predicted to increase in the Klamath Mountains and North Cascades. Large percentages of forest also transitioned from low and moderate to higher suitability in the Northern Rockies and East Cascades.

4.2. Fire rotation periods under climate change

Fire rotation periods varied widely across the study area and through time. Given the recent increase in numbers of large forest wildfires and extent of area burned (Fig. 2) the FRPs of the current climate normal were less than they were for the baseline period.

However, the relative FRP differences between large wildfire suitability classes remained relatively stable between time periods. Using these relative class differences, the predicted relative magnitude of FRP shortening was greatest in the moister/cooler forested ecoregions and lesser, but still shortened, in the warmer/drier ecoregions by the end of this century. Given that FRP is inversely related to area burned, the results in Table 3 corroborate those by Littell et al. (2010) who modeled a two- or three-fold increase in annual area burned in Washington forests under various climate change scenarios. Similarly, a study by Rogers et al. (2011) showed a 0.8–3.1 increase in annual area burned for Oregon and Washington (including non-forested areas) by the end of the 21st century. Rogers et al. (2011) also modeled larger proportional increases in future percent area burned per year in moister forests west of the Cascade Crest in Oregon and Washington than in drier forests east of it. Our modeling indicated that the FRPs in forests of the coastal ecoregions will remain fairly stable to the end of this century, relative to other areas. We suspect this is likely due to a buffering of climate from the Pacific Ocean's maritime influence. However, there were smaller geographic areas in other ecoregions where FRPs were estimated to remain relatively stable, likely do to topographic influences (Fig. 10).

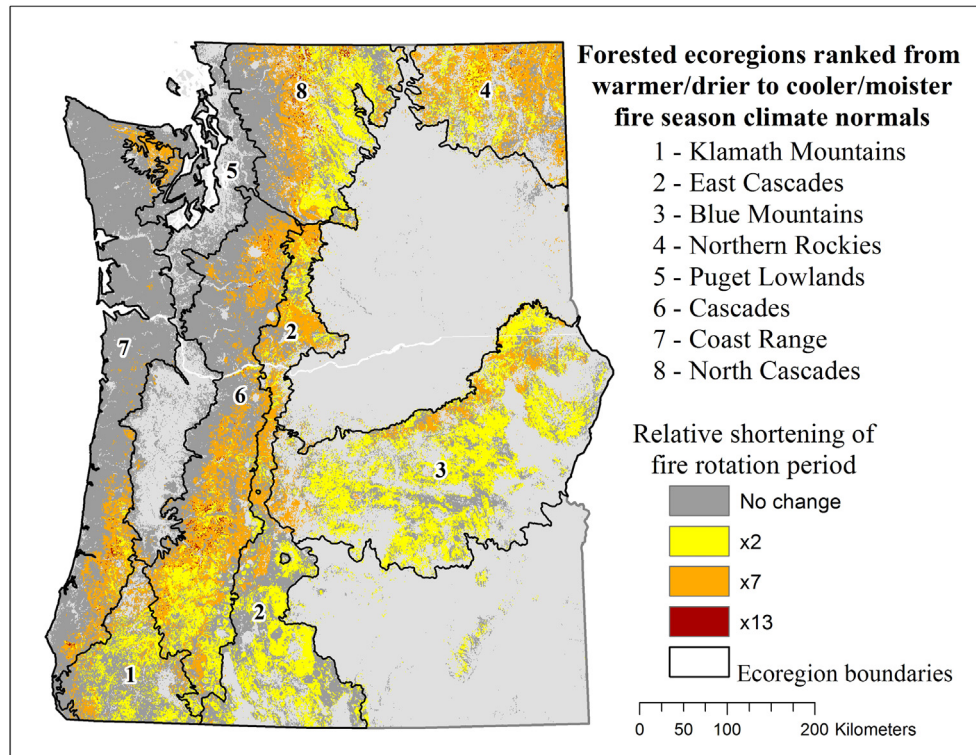


Fig. 10. Estimated changes in fire rotation periods by the end of this century.

There are several existing studies that have already shown or predicted increasing trends of wildfire as a result of climate change (Barbero et al., 2015; Dennison et al., 2014; Moritz et al., 2012; Rogers et al., 2011; Stavros et al., 2014; West et al., 2016; Westerling, 2016). This study adds to that list, but was confined specifically to the forested ecosystem to avoid confounding environmental factors that control large wildfires differently in non-forested ecosystems. Moreover, our results highlighted the divergent sensitivity of differing forested ecoregions and ownerships to climate-induced increases in forest wildfire suitability. This study also provided a finer scale regional focus and a time series of map products that illustrate how the changing geography of forest wildfire suitability might proceed through this century.

4.3. Model uncertainty and limitations

While climate is an important environmental control for large wildfires, other factors can and do modify the fire environment

Table 3
Mean fire rotation period (FRP) relative shortening factors by geographic area. Standard deviations in parenthesis.

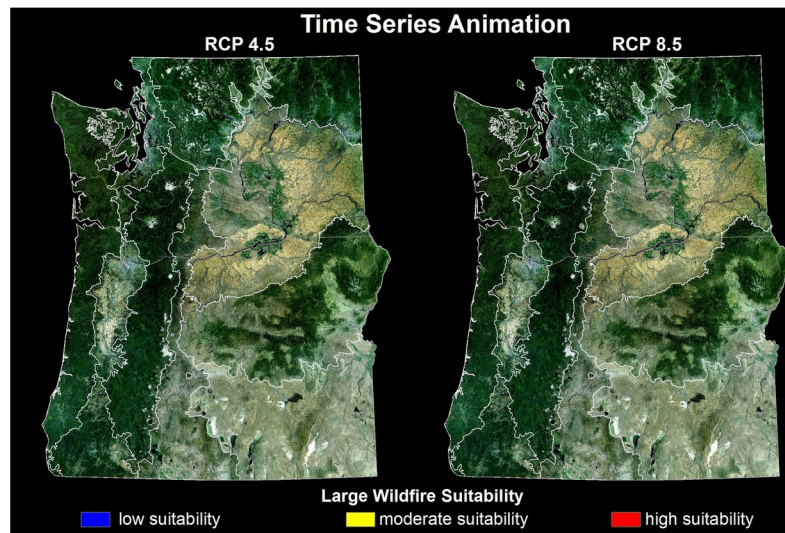
Geographic area	RCP 4.5	RCP 8.5
Forested ecoregion		
Northern Rockies	3.6 (3.3)	4.1 (3.2)
Cascades	2.3 (3.1)	2.5 (3.2)
North Cascades	2.2 (2.9)	2.5 (3.0)
East Cascades	2.0 (2.7)	2.2 (2.7)
Blue Mountains	1.7 (2.0)	1.9 (2.0)
Klamath Mountains	1.5 (2.4)	1.6 (2.4)
Coast Range	0.8 (2.3)	0.9 (2.4)
Puget Lowlands	0.1 (0.7)	0.1 (0.7)
Forest ownership		
USDI Bureau of Land Management	3.1 (1.7)	3.5 (1.8)
USDA Forest Service	2.9 (1.4)	3.3 (1.6)
Tribal	2.5 (1.2)	2.8 (1.5)
Private	2.0 (1.3)	2.2 (1.6)
USDI National Park Service	1.9 (1.1)	2.0 (1.3)
State and Local	1.6 (1.1)	1.8 (1.4)

at finer spatial and temporal scales (Krawchuk and Moritz, 2014; Littell et al., 2016; Mann et al., 2016). For example, wildfire effects that remove or reduce burnable forest fuels may modify large wildfire suitability for years following a fire. Likewise, so might fuels reduction programs that reduce fuels or break up their continuity prior to an ignition. These feedback mechanisms and human factors may serve to temporally dampen the environmental suitability for large wildfires for a period of time, and should be considered when using the maps produced here. Similarly, these models and maps are representations of 30-year weather averages that represent the conditions normally expected to occur and do not represent the annual variation between the cooler/moister and hotter/drier years—when most large wildfires in this region occur (Littell et al., 2009). Additionally, our modeling assumed that the forested area of today remains stable throughout this century. However, this may not be the case if post-disturbance forest diebacks occur in areas where the climate can no longer support forest redevelopment (Allen et al., 2015; Clark et al., 2016).

The use of clamping in our climate response functions indicated it could dampen relative fire suitability predictions when TMAX exceeds 32.4 °C (Fig. 6a). Given the high relative suitability where TMAX clamping occurs (0.76), we suspect our projected models may slightly under predict mostly the high suitability map class for later climate normals, especially under RCP 8.5. The spatial extent of this novel predicted future temperature condition did not exceed 5% of the forested areas until the 2041–2070 climate normal period (under RCP 8.5). It mostly occurred along the lower elevation forest/nonforest margins in southwest Oregon and east of the Cascades. We suspect that these forest margins may be the first areas to experience dieback. However, increased precipitation, changes in tree physiology due to increased levels of CO₂, and other environmental factors will play a role in how this complex process unfolds (Allen et al., 2015). How these potential environmental changes will affect the overall geographic patterns of future forests and large wildfire suitability remains an area for active monitoring and research.

Finally, our models only relate to fire occurrence and not fire severity. Forests modeled as normally having low suitability for large wildfire occurrence contain fuel conditions predisposed for the relatively infrequent, yet extremely large and severe wildfire events that occur during conditions of very extreme drought and altered synoptic weather patterns as witnessed by past events such as the Tillamook Burn of 1933 (Agee, 1993). The modeling here,

the 21st century. These maps are easily interpreted and may prove useful for planning of short and long-term forest fire and fuels management (Millar et al., 2007; Thompson et al., 2013), informing urban planning and development in forest interfaces (Fernandes, 2013; Syphard et al., 2013), forest reserve network designs (Berry et al., 2015; Mackey et al., 2012), and forest carbon management (Fonseca et al., 2016).



Animation 1. LWS time series animation.

and the maps produced, only addressed normal intrinsic fire environments and not abnormal conditions and events.

5. Conclusion

In 2015 the US Northwest Climate Division and our study area had its warmest fire season on record in over a century (<http://www.ncdc.noaa.gov/>) and experienced its highest number of large wildfires and forests burned since 1971 (Fig. 2). Our modeling indicated that if the climate continues to change as predicted, it will likely result in an increase of Pacific Northwest forests with fire season environments more suitable for the occurrence of large forest wildfires. As low suitability forests shrink in area and high suitability forests expand, there will likely be a continued shortening of fire rotation periods in the study area and large forest wildfires will become more commonplace (or normal) in the future. The increase in forest vulnerability to large forest wildfires and shortening of fire rotations was more pronounced under the RCP 8.5 scenario.

Based on a recent study, our study area incurs the highest per fire suppression costs in the United States (Gebert et al., 2007). Most of these costs are spent on the large wildfires. Thus, as the frequency of large wildfires increases, the annual cost of suppression would also be expected to increase. However, shifts in fire suppression strategies might result in substantially lower annual suppression costs that could help offset those potential increases (Houtman et al., 2013).

Aside from wildfire suppression considerations, the time series maps produced herein (LWS Time Series) offer natural resource management agencies, fire protection districts, and policy-makers empirical and validated estimates and visualizations of how climate change might affect current geographic patterns of large wildfire within the forests of Oregon and Washington for

Fire was and remains a natural process in these forests (Agee, 1993), and these fire environment maps may contribute to our understanding of how (geographically) it normally fits into the ecosystem now, and into the near future. The leading edges of change, where one forest suitability class was predicted to transition into the next higher class, will likely be the areas where the effects of climate change on large wildfire occurrence may be observed first (Whitman et al., 2015). Increasing environmental suitability for large wildfire occurrence had differing effects on fire rotation periods, with moister/cooler forests experiencing larger FRP decreases than warmer/drier forests. Thus; the magnitude of change, in terms of forest area burned and the social, ecological, and economic ramifications that go with that, will likely be higher in low suitability forests that transition into moderate or high suitability. Low wildfire suitability areas that remained temporally constant in our modeling might serve as focal areas for fire refugia and reserves designed to maintain or restore older, denser, closed-canopy forests. Forest that are currently classified as moderate suitability or are predicted to transition into it may be places to focus active management to improve forest resilience to future wildfires. Where forests have or are predicted to transition into higher wildfire suitability classes and, due to their juxtaposition, also pose threats to infrastructure, valued forest resources, or areas of conservation concern and where fire has not been as common may need management attention to ameliorate fire risks.

Acknowledgements

Partial funding of this analysis was provided by Oregon Department of Forestry. Climate scenarios used were from the NEX-DCP30 dataset, prepared by the Climate Analytics Group and NASA Ames Research Center using the NASA Earth Exchange, and distributed by the NASA Center for Climate Simulation (NCCS).

References

- Abatzoglou, J.T., Williams, A.P., 2016. Impact of anthropogenic climate change on wildfire across western US forests. *Proc. Natl. Acad. Sci.* 113 (42), 11770–11775.
- Agee, J.K., 1993. *Fire Ecology of Pacific Northwest Forests*. Island Press, Washington, DC.
- Alexander, M.E., Cruz, M.G., 2013. Are the applications of wildland fire behavior models getting ahead of their evaluation again? *Environ. Model. Softw.* 41, 65–71.
- Allen, C.D., Breshears, D.D., McDowell, N.G., 2015. On underestimation of global vulnerability to tree mortality and forest die-off from hotter drought in the Anthropocene. *Ecosphere* 6 (8), 129.
- Arroyo, L.A., Pascual, C., Manzanera, J.A., 2008. Fire models and methods to map fuel types: the role of remote sensing. *For. Ecol. Manage.* 256, 1239–1252.
- Barbero, R., Abatzoglou, J.T., Steel, E.A., Larkin, N.K., 2014. Modeling very large-fire occurrence over the continental United States from weather and climate forcing. *Environ. Res. Lett.* 9, 124009.
- Barbero, R., Abatzoglou, J.T., Larkin, N.K., Kolden, C.A., Stocks, B., 2015. Climate change presents increased potential for very large fires in the contiguous United States. *Int. J. Wildl. Fire* 24, 892–899.
- Beatty, R.M., Taylor, A.H., 2001. Spatial and temporal variation of fire regimes in a mixed conifer forest landscape, southern Cascades, California, USA. *J. Biogeogr.* 28, 955–966.
- Bell, D.M., Schlaepfer, D.R., 2016. On the dangers of model complexity without ecological justification in species distribution modeling. *Ecol. Model.* 330, 50–59.
- Berry, L.E., Driscoll, D.A., Stein, J.A., Blanchard, W., Banks, S.C., Bradstock, R.A., Lindenmayer, D.B., 2015. Identifying the location of fire refuges in wet forest ecosystems. *Ecol. Appl.* 25, 2337–2448.
- Boyce, M.S., Vernier, P.R., Nielsen, S.E., Schmiegelow, F.K., 2002. Evaluating resource selection functions. *Ecol. Model.* 157, 281–300.
- Burnham, K.P., Anderson, D.R., 2002. *Model Selection and Multimodel Inference: A Practical Information-Theoretic Approach*. Springer-Verlag, New York.
- Byers, R.C., Steinhorst, R.K., Krausman, P.R., 1984. Clarification of a technique for analysis of utilization-availability data. *J. Wildl. Manage.* 48 (3), 1050–1053.
- Clark, J.S., Iverson, L., Woodall, C.W., Allen, C.D., Bell, D.M., Bragg, D.C., D'Amato, A. W., Davis, F.W., Hersh, M.H., Ibanez, I., Jackson, S.T., Matthews, S., Pederson, N., Peters, M., Schwartz, M.W., Waring, K.M., Zimmermann, N.E., 2016. The impacts of increasing drought on forest dynamics, structure, and biodiversity in the United States. *Glob. Change Biol.* 22, 2329–2352.
- Clarke, P.J., 2002. Habitat islands in fire-prone vegetation: do landscape features influence community composition? *J. Biogeogr.* 29, 1–8.
- Countryman, C.M., 1972. *The Fire Environment Concept*. USDA Forest Service, Pacific Southwest Forest and Range Experiment Station, Berkeley. 12 p.
- Daly, C., Halbleib, M., Smith, J.L., Gibson, W.P., Doggett, M.K., Taylor, G.H., Curtis, J., Pasteris, P.A., 2008. Physiographically-sensitive mapping of temperature and precipitation across the conterminous United States. *Int. J. Clim.* 28, 2031–2064.
- Davis, R.J., Aney, W.C., Evers, L., Dugger, K.M., 2011. Large wildfires within the owl's range. In: *Northwest Forest Plan—The First 15 Years (1994–2008): Status and Trends of Northern Spotted Owl Populations and Habitats*. Gen. Tech. Rep. PNW-GTR-850. USDA, Forest Service, Pacific Northwest Research Station, Portland, OR, 147 p. (Chapter 4).
- De Angelis, A., Ricotta, C., Conedera, M., Pezzatti, G.B., 2015. Modelling the meteorological forest fire niche in heterogeneous pyrologic conditions. *PLoS ONE* 10 (2), e0116875. <http://dx.doi.org/10.1371/journal.pone.0116875>.
- Dennison, P.E., Brewer, S.C., Arnold, J.D., Moritz, M.A., 2014. Large wildfire trends in the western United States, 1984–2011. *Geophys. Res. Lett.* 41, 2928–2933.
- Dissing, D., Verbyla, D.L., 2003. Spatial patterns of lightning strikes in interior Alaska and their relations to elevation and vegetation. *Can. J. For. Res.* 33, 770–782.
- Dormann, C.F., Elith, J., Bacher, S., Buchmann, C., Carl, G., Carré, G., Marquéz, J.R.G., Gruber, B., Lafourcade, B., Leitão, P.J., Münkemüller, T., McClean, C., Osborne, P. E., Reineking, B., Schröder, B., Skidmore, A.K., Zurell, D., Lautenbach, S., 2013. Collinearity: a review of methods to deal with it and a simulation study evaluating their performance. *Ecography* 36, 027–046.
- Elith, J., Phillips, S.J., Hastie, T., Dudík, M., Chee, Y.E., Yates, C.J., 2011. A statistical explanation of MaxEnt for ecologists. *Divers. Distrib.* 17, 43–57.
- Ellison, A., Mosely, C., Evers, C., Nielsen-Pincus, M., 2013. *Forest Service Spending on Large Wildfires in the West*. Working Paper 41. Ecosystem Workforce Program, University of Oregon, Eugene, OR, 16 p. <https://www.firescience.gov/projects/09-1-10-3/project/09-1-10-3_WP_41.pdf>.
- Fernandes, P.M., 2013. Fire-smart management of forest landscapes in the Mediterranean basin under global change. *Landsc. Urban Plan.* 110, 175–182.
- Fielding, A.H., Bell, J.F., 1997. A review of methods for the assessment of prediction errors in conservation presence/absence models. *Environ. Conserv.* 24, 38–49.
- Flannigan, M.D., Stocks, B.J., Wotton, B.M., 2000. Climate change and forest fires. *Sci. Total Environ.* 262, 221–229.
- Fonseca, M.G., Aragaõ, L.E.O.C., Lima, A., Shimabukuro, Y.E., Arai, E., Anderson, L.O., 2016. Modelling fire probability in the Brazilian Amazon using the maximum entropy method. *Int. J. Wildl. Fire* 25, 955–969.
- Gebert, K.M., Calkin, D.E., Yoder, J., 2007. Estimating suppression expenditures for individual large wildland fires. *West. J. Appl. For.* 22, 188–196.
- Gorelick, N., 2013. Google earth engine. EGU Gen. Assemb. Conf. Abstr. 15, 11997 <<http://meetingorganizer.copernicus.org/EGU2013/EGU2013-11997.pdf>>.
- Hirzel, A.H., LeLay, G., Helfer, V., Randin, C., Guisan, A., 2006. Evaluating the ability of habitat suitability models to predict species presences. *Ecol. Model.* 199 (2), 142–152.
- Houtman, R.M., Montgomery, C.A., Gagnon, A.R., Calkin, D.E., Dietterich, T.G., McGregor, S., Crowley, M., 2013. Allowing a wildfire to burn: estimating the effect on future wildfire suppression costs. *Int. J. Wildl. Fire* 22 (7), 871–882.
- Hustich, I., 1978. A change in attitudes regarding the importance of climatic fluctuations. *Fennia* 150, 59–65.
- Keane, R.E., 2013. Describing wildland surface fuel loading for fire management: a review of approaches, methods and systems. *Int. J. Wildl. Fire* 22, 51–62.
- Krawchuk, M.A., Moritz, M.A., Parisien, M.-A., Van Dorn, J., Hayhoe, K., 2009. Global pyrogeography: the current and future distribution of wildfire. *PLoS ONE* 4 (4), e5102.
- Krawchuk, M.A., Moritz, M.A., 2014. Burning issues: statistical analyses of global fire data to inform assessments of environmental change. *Environmetrics* 25, 472–481.
- Li, C., 2002. Estimation of fire frequency and fire cycle: a computational perspective. *Ecol. Model.* 154, 103–120.
- Littell, J.S., McKenzie, D., et al., 2009. Climate, wildfire area burned in western US ecoregions, 1916–2003. *Ecol. Appl.* 19, 1003–1021.
- Littell, J.S., Oneil, E.E., McKenzie, D., Hicke, J.A., Lutz, J.A., Norheim, R.A., Elsner, M.M., 2010. Forest ecosystems, disturbance, and climatic change in Washington State, USA. *Clim. Change* 102, 129–158.
- Littell, J.S., Peterson, D.L., Riley, K.L., Liu, Y., Luce, C.H., 2016. A review of the relationships between drought and forest fire in the United States. *Glob. Change Biol.* <http://dx.doi.org/10.1111/gcb.13275>.
- Liu, Z., Wimberly, M.C., 2016. Direct and indirect effects of climate change on projected future fire regimes in the western United States. *Sci. Total Environ.* 542(A), 65–75.
- Lutz, J.A., Key, C.H., Kolden, C.A., Kane, J.T., van Wagtenonk, J.W., 2011. Fire frequency, area burned, and severity: a quantitative approach to defining a normal fire year. *Fire Ecol.* 7, 51–65.
- Mackey, B.G., Berry, S., Hugh, S., Ferrier, S., Harwood, T., Williams, K., 2012. Ecosystem greenspots: identifying potential drought, fire and climate change micro-refuges. *Ecol. Appl.* 22, 1852–1864.
- Mann, M.L., Battlori, E., Moritz, M.A., Waller, E.K., Berck, P., Flint, A.L., Flint, L.E., Dolff, E., 2016. Incorporating anthropogenic influences into fire probability models: effects of human activity and climate change on fire activity in California. *PLoS ONE* 11 (4). <http://dx.doi.org/10.1371/journal.pone.0153589>.
- McKenzie, D., Gedalof, Z., Peterson, D.L., Mote, P., 2004. Climatic change, wildfire, and conservation. *Conserv. Biol.* 18 (4), 890–902.
- Merow, C., Smith Jr., M.J., Silander, J.A., 2013. A practical guide to MaxEnt for modeling species' distributions: what it does, and why inputs and settings matter. *Ecography* 36, 1058–1069.
- Merow, C., Smith Jr., M.J., Edwards, T.C., Guisan, A., McMahon, S.M., Normand, S., Thuiller, W., Wüest, R.O., Zimmermann, N.E., Elith, J., 2014. What do we gain from simplicity versus complexity in species distribution models? *Ecography* 37, 267–281.
- Millar, C.I., Stephenson, N.L., Stephens, S.L., 2007. Climate change and forests of the future: managing in the face of uncertainty. *Ecol. Appl.* 17, 2145–2151.
- Moreira, F., Rego, F.C., Ferreira, P.G., 2001. Temporal (1958–1995) pattern of change in a cultural landscape of northwestern Portugal: implications for fire occurrence. *Landsc. Ecol.* 16, 557–567.
- Moritz, M.A., Parisien, M.-A., Battlori, E., Krawchuk, M.A., Van Dorn, J., Ganz, D.J., Hayhoe, K., 2012. Climate change and disruptions to global fire activity. *Ecosphere* 3 (6), 49.
- Moritz, M.A., Battlori, E., Bradstock, R.A., Gill, A.M., Handmer, J., Hessburg, P.F., Leonard, J., McCaffrey, S., Odion, D.C., Schoennagel, T., 2014. Learning to coexist with wildfire. *Nature* 515, 58–66.
- Mote Jr., P.W., Salathe, E.P., 2010. Future climate in the Pacific Northwest. *Clim. Change* 102, 29–50.
- Nemani, R., Votava, P., Michaelis, A., Melton, F., Milesi, C., 2011. Collaborative supercomputing for global change science. *EOS Trans. Am. Geophys. Union* 92 (13), 109–110.
- North, M.P., Stephens, S.L., Collins, B.M., Agee, J.K., Aplet, G., Franklin, J.F., Zule, P.Z., 2015. Reform forest fire management; agency incentives undermine policy effectiveness. *Science* 349, 1280–1281.
- Omernik, J.M., Griffith, G.E., 2014. Ecoregions of the conterminous United States: evolution of a hierarchical spatial framework. *Environ. Manage.* 54, 1249–1266.
- Parisien, M.-A., Moritz, M.A., 2009. Environmental controls on the distribution of wildfire at multiple spatial scales. *Ecol. Monogr.* 79, 127–154.
- Parisien, M.-A., Snetsinger, S., Greenberg, J.A., Nelson, C.R., Schoennagel, T., Dobrowski, S.Z., Moritz, M.A., 2012. Spatial variability in wildfire probability across the western United States. *Int. J. Wildl. Fire* 21, 313–327.
- Peterson, D.W., Kerns, B.K., Dodson, E.K., 2014. *Climate Change Effects on Vegetation in the Pacific Northwest: A Review and Synthesis of the Scientific Literature and Simulation Model Projections*. Gen. Tech. Rep. PNW-GTR-900. USDA, Forest Service, Pacific Northwest Research Station, Portland, OR, 183 p.
- Phillips, S.J., Anderson, R.P., Schapire, R.E., 2006. Maximum entropy modeling of species geographic distributions. *Ecol. Model.* 190, 231–259.
- Phillips, S.J., Dudík, M., 2008. Modeling of species distributions with MaxEnt: new extensions and a comprehensive evaluation. *Ecography* 31 (2), 161–175.
- Preisler, H.K., Brillinger, D.R., Burgan, R.E., Benoit, J.W., 2004. Probability based models for estimation of wildfire risk. *Int. J. Wildl. Fire* 13, 133–142.

- PRISM, 2015. PRISM Climate Group, Oregon State University <<http://prism.oregonstate.edu>> (accessed 15.02.12).
- Purves, D., Pacala, S., 2008. Predictive models of forest dynamics. *Science* 320, 1452–1453.
- Reifsnyder, W.E., 1960. Weather and fire control practices. In: *Proceedings of the Fifth World Forestry Congress*, vol. 2. University of Washington, Seattle, Washington, USA, pp. 835–841.
- Riahi, K., Rao, S., Krey, V., Cho, C., Chirkov, V., Fischer, G., Kindermann, G., Nakicenovic, N., Rafaj, P., 2011. RCP 8.5—a scenario of comparatively high greenhouse gas emissions. *Clim. Change* 109, 33–57.
- Rogers, B.M., Neilson, R.P., Drapek, R., Lenihan, J.M., Wells, J.R., Bachelet, D., Law, B. E., 2011. Impacts of climate change on fire regimes and carbon stocks of the US Pacific Northwest. *J. Geophys. Res.* 116 (G3).
- Ruefenacht, B., Finco, M.V., Nelson, M.D., Czaplowski, R., Helmer, E.H., Blackard, J.A., et al., 2008. Conterminous U.S. and Alaska forest type mapping using forest inventory and analysis data. *Photogr. Eng. Rem. Sens.* 74, 1379–1388.
- Stavros, E.N., Abatzoglou, J., Larkin, N.K., McKenzie, M., Steel, E.A., 2014. Climate and very large wildland fires in the contiguous Western USA. *Int. J. Wildl. Fire* 23, 899–914.
- Swets, J.A., 1988. Measuring the accuracy of diagnostic systems. *Science* 240, 1285–1293.
- Syphard, A.D., Bar Massada, A., Butsic, V., Keeley, J.E., 2013. Land use planning and wildfire: development policies influence future probability of housing loss. *PLoS ONE* 8 (8). <http://dx.doi.org/10.1371/journal.pone.0071708>.
- Taylor, K.E., Stouffer, R.J., Meehl, G.A., 2012. An overview of CMIP5 and the experiment design. *Bull. Am. Meteorol. Soc.* 93, 485–498.
- Thompson, M.P., Calkin, D.E., Finney, M.A., Gebert, K.M., Hand, M.S., 2013. A risk-based approach to wildland fire budgetary planning. *For. Sci.* 59, 63–77.
- Thomson, A., Calvin, K.V., Smith, S.J., Kyle, G.P., Volke, A., Patel, P., Delgado-Arias, S., Bond-Lamberty, B., Wise, M.A., Clarke, L.E., Edmonds, J.A., 2011. RCP4.5: a pathway for stabilization of radiative forcing by 2100. *Clim. Change* 109, 77–94.
- Thrasher, B., Xiong, J., Wang, W., Melton, F., Michaelis, A., Nemani, R., 2013. New downscaled climate projections suitable for resource management in the U.S. *EOS Trans. Am. Geophys. Union* 94, 321–323.
- Trewin, B., 2007. *The Role of Climatological Normals in a Changing Climate*. WMO-TD No. 1377. World Meteorological Organization, Geneva, 46 p. <https://www.wmo.int/datastat/documents/WCDMPNo61_1.pdf>.
- USDA, 2015. *The Rising Cost of Fire Operations: Effects on the Forest Service's Non-fire Work*. US Department of Agriculture, Forest Service. 16 p. <<http://www.fs.fed.us/sites/default/files/2015-Fire-Budget-Report.pdf>>.
- Van Vuuren, D.P., Edmonds, J., Kainuma, M., Riahi, K., Thomson, A., Hibbard, K., Hurtt, G.C., Kram, T., Krey, V., Lamarque, J.F., Masui, T., Meinshausen, M., Nakicenovic, N., Smith, S.J., Rose, S.K., 2011. The representative concentration pathways: an overview. *Clim. Change* 109, 5–31.
- van Wageningen, J.W., Cayan, D.R., 2008. Temporal and spatial distribution of lightning strikes in California in relation to large-scale weather patterns. *Fire Ecol.* 4 (1), 34–56.
- West, A.M., Kumar, S., Jarnevich, C.S., 2016. Regional modeling of large wildfires under current and potential future climates in Colorado and Wyoming, USA. *Clim. Change* 134, 565–577.
- Westerling, A.L.R., 2016. Increasing western US forest wildfire activity: sensitivity to changes in the timing of spring. *Philos. Trans. R. Soc. B* 371, 20150178. <http://dx.doi.org/10.1098/rstb.2015.0178>.
- Whitman, E., Battlori, E., Parisien, M.-A., Miller, C., Coop, J.D., Krawchuk, M.A., Chong, G.W., Haire, S.L., 2015. The climate space of fire regimes in north-western North America. *J. Biogeogr.* 42, 1736–1749.